Diagnostic performance and impact on patient management of [68Ga]Ga-DOTA-TOC PET/CT in colorectal neuroendocrine tumors derived from hindgut

Pierre Delabie, MD[a] , Éric Baudin, MD, PhD[b], Olivia Hentic, MD[c], Pauline Afchain, MD[d], Timofei Rusu, MD[a], Françoise Montravers, MD, PhD[a]

Abstract

The main purpose of this retrospective study was to determine the diagnostic performance of [68Ga]Ga-DOTA-D-Phe1-Try3-octreotide(DOTA-TOC) positron emission tomography/computed tomography (PET/CT) in patients with well-differentiated colorectal Neuroendocrine Tumours (NETs) originating from the hindgut. The other aims were to assess the impact of the examination on patient management and to analyze the results of 2-[18F]FDG and/or 6-[18F]FDOPA PET/CT when they were performed. [68Ga]Ga-DOTA-TOC PET/CT and clinical data from 30 patients with biopsy-proven well-differentiated NETs originating from the hindgut were retrospectively reviewed and analyzed by comparing the [68Ga]Ga-DOTA-TOC PET/CT findings with pathological and/or follow-up data. We also compared the [68Ga]Ga-DOTA-TOC PET/CT results with 2-[18F]FDG and/or 6-[18F]FDOPA PET/CT results in 6 patients. The impact on management was determined in hindsight by comparing the patient management decided before and after the TEP examination based on data from multidisciplinary team meetings. On a patient basis, [68Ga]Ga-DOTA-TOC PET/CT was accurate in 30 of the 30 examinations. [68Ga]Ga-DOTA-TOC PET/CT correctly identified the primary tumor in all patients with primary tumors not resected before the examination and allowed the detection of unexpected distant metastases in 36% of the patients referred for initial staging. [68Ga]Ga-DOTA-TOC PET/CT findings affected patient management in 57% of cases with generally major intermodality changes. Intraindividual comparison of the results of the different PET radiopharmaceuticals showed a clear superiority of [68Ga]Ga-DOTA-TOC PET/CT considering both the number of lesions and the intensity of uptake. [68Ga]Ga-DOTA-TOC PET/CT is an accurate imaging modality for the assessment of well-differentiated colorectal NETs that highly impact patient management. Thus, we suggest that [68Ga]Ga-DOTA-TOC PET/CT be employed as a first choice for the assessment of these tumors in nuclear medicine.

Abbreviations: ^{18}F = Fluorine-18, ^{68}Ga = Gallium-68, ^{68}Ge = Germanium-68, DOTA-TOC = DOTA-$_D$-Phe^1-Try^3-octreotide, FOV = field of view, IQR = interquartile range, NETs = Neuroendocrine Tumours, PET/CT = positron emission tomography/computed tomography, PI = proliferative index, PL = peritoneal lesion, PRRT = peptide receptor radionuclide therapy, SR = somatostatin receptors, SSA = somatostatin analogue, SUV_{max} = maximum standardized uptake value, TP = true positive

Keywords: colorectal, neuroendocrine tumours, oncology, PET imaging, somatostatin receptors

1. Introduction

Colorectal neuroendocrine tumors (NETs) originating from the hindgut correspond to NETs located from the last third of the transverse colon to the rectum. They are relatively uncommon, accounting for ~20% of all NETs, and are mostly discovered incidentally during routine surveillance endoscopies.[1] They are rarely, if ever, associated with a hormonal syndrome such as flushing or diarrhea, even in the metastatic stage.[1] Other clinical symptoms that may occur include rectal bleeding, pain and changes in bowel habits.[2,3] Surgery is the mainstay for the treatment of local or locoregional colorectal NETs, while systemic therapies such as somatostatin analogues (SSA) or chemotherapy are indicated to treat advanced/metastatic disease.[4,5] Peptide receptor radionuclide therapy (PRRT) may be a potential treatment in well-selected patients with metastatic rectal NETs.[6]

Accurate staging is important for the determination of resectability and prognosis, particularly for primary tumors larger than 1 cm,[5] but the small size and variable anatomic location of metastases may limit their detection in imaging. Overexpression of cell-surface somatostatin receptors (SR) – in particular of SR type 2 (SR2) – is a feature of well-differentiated NETs, enabling functional imaging with radiolabelled SSA.[7,8] Therefore, somatostatin receptor positron emission tomography (SR PET) has been widely documented in NETs, with a superior diagnostic performance compared with that of somatostatin receptor scintigraphy.[9,10] Several SSA for SR PET labeled with gallium-68 using a 1,4,7,10-tetraazacyclododecane-1,4,7,10-tetra-acetic acid (DOTA) cage have been evaluated with a comparable diagnostic accuracy[11]: DOTA-$_D$-Phe[1]-Try[3]-octreotide (DOTA-TOC), DOTA-$_D$-Phe[1]-Try[3]-octreotate, and DOTA-1-NaI-Try[3]-octreotide. Furthermore, some NETs can take up and decarboxylate monoamine precursors such as dihydroxyphenylalanine, allowing their possible detection on 6-[18F]FDOPA PET.[12] Fluorine-18 fluoro-2-D-deoxyglucose (2-[18F]FDG) better detects highly metabolic neuroendocrine carcinomas than well-differentiated tumors but may, however, have diagnostic and prognostic value in well-differentiated NETs.[13–15]

In 2017, Bozkurt et al.[16] proposed a diagnostic strategy specific to hindgut NETs with the use of 2-[18F]FDG Positron Emission Tomography/Computed Tomography (PET/CT) as the first choice and 6-[18F]FDOPA or [68Ga]Ga-DOTA-peptide PET/CT as the equivalent second choice. In 2018, the revision of the Society of Nuclear Medicine and Molecular Imaging practice guidelines recommended SR PET as the initial functional imaging modality for the diagnosis of well-differentiated NETs regardless of their origin.[17] More recently, the National Comprehensive Cancer Network® (NCCN Guidelines®) defined the use of SR PET for the evaluation of rectal NETs as appropriate.[18] Nevertheless, more recently, the study by Zhou et al.[19] showed that [68Ga]Ga-DOTA-NOC PET-CT was a promising tool for detecting lymph node metastasis in rectal NETs with high sensitivity and specificity and better results than 2-[18F]FDG PET-CT.

The main aims of this retrospective study were to determine the diagnostic performance of [68Ga]Ga-DOTA-TOC PET/CT in consecutive patients referred to our center for the assessment of well-differentiated NETs derived from the hindgut (including rectal and colic NETs) and to evaluate its impact on patient management. The secondary objectives were to compare the results of [68Ga]Ga-DOTA-TOC PET/CT to those of 2-[18F]FDG and/or 6-[18F]FDOPA PET/CT when performed and to search for a correlation between the value of the Ki-67 proliferative index (PI) of surgically resected or biopsied lesions and the intensity of their uptake on [68Ga]Ga-DOTA-TOC PET/CT quantified by the maximum standardized uptake value (SUV$_{max}$).

2. Materials and methods

2.1. Study population

We retrospectively analyzed all consecutive patients referred to our nuclear medicine department between September 2009 and July 2020 for [68Ga]Ga-DOTA-TOC PET/CT.

The inclusion criteria for patients were as follows:

1. histologically confirmed well-differentiated digestive NET (NET G1, G2 or G3 according to the 2019 World Health Organization grading system[20]) originating from the hindgut
2. age greater than 18 years
3. follow-up data available

The exclusion criteria for patients were as follows:

1. digestive NET originating from the midgut or the foregut
2. NEC or other histological diagnosis than a neuroendocrine neoplasia

Whether patients underwent 2-[18F]FDG and/or 6-[18F]FDOPA PET/CT at the time of [68Ga]Ga-DOTA-TOC PET/CT was recorded (flow diagram, Fig. 1). We only kept for comparison any PET/CT performed with an interval between examinations less than 30 days except for 1 patient with a longer delay of 6 months (patient no. 6), which was acceptable due to the absence of change in therapeutic management between the PET examinations and the slow growth of the disease.

As [68Ga]Ga-DOTA-TOC was not yet registered in France until December 2016, PET/CTs were performed through the compassionate use program authorized on an individual basis by the French National Agency for Drug and Health Product Safety (ANSM) before the registration date. This research implied no intervention for the patient. According to French regulations, the approval of an institutional review board was not necessary for performing this retrospective analysis of already-available data. Regardless of the date of examination, patients were informed that their data collected for the [68Ga]Ga-DOTA-TOC PET/CT would be analyzed anonymously, and they did not object.

2.2. [68Ga]Ga-DOTA-TOC PET/CT imaging procedure

2.2.1. Acquisition protocol. DOTA-TOC was radiolabelled with [68Ga]Ga in the radiopharmacy of our nuclear medicine department. [68Ga]Ga was eluted from a commercially available [68Ge]Ge/[68Ga]Ga radionuclide generator (GalliaPharm Eckert & Ziegler Radiopharma GmBH) prior to DOTA-TOC radiolabelling following the Breeman procedure.[21] No specific preparation of the patient was required before the radiotracer was injected. Patients received 1 to 2 MBq/kg of body mass of [68Ga]Ga-DOTA-TOC injected via an infusion line connected to saline. For patients treated with SSA, medication was not discontinued before the imaging procedure.

Head-to-mid-thigh PET/CT imaging was performed 45 to 90 minutes after injection either on Gemini TF16 PET/CT (Philips Healthcare®) or on Biograph mCTflow (Siemens Healthcare®) PET/CT, both equipped with time-of-flight technology.

The characteristics for Gemini TF16 PET/CT were as follows: 3D mode, 576 mm field of view (FOV), and 144 × 144 matrix. Images were reconstructed using the OSEM weighted method based on 3 iterations and 33 subsets; low-dose CT without contrast enhancement was performed prior to PET acquisition (120 kVp, 80 mA.s, slice thickness: 2.5 mm, pitch: 0.813, rotation time: 0.5 seconds, and FOV: 600 mm) for attenuation correction and anatomic localization.

The characteristics for Biograph mCTflow were as follows: 3D mode, 780 mm FOV, and 200 × 200 matrix. Those images were reconstructed using the OSEM weighted method based on 2 iterations and 21 subsets; low-dose CT without contrast enhancement was performed prior to PET acquisition (CareDose® automatic modulation for keV and mA.s, slice thickness: 2 mm, pitch: 0.813, rotation time: 0.5 seconds, and FOV: 500 mm).

On both machines, the imaging time was 2 minutes per bed position.

2.2.2. Image analysis and endpoints. PETs were read by 1 nuclear medicine specialist aware of the results of the other imaging modalities using the Carestream Vue picture archiving and communication system (Carestream Health, Inc, Rochester, NY). Any focus with a visual intensity greater than background and that could not be explained by physiologic uptake (e.g., pituitary gland, spleen, liver, adrenal glands, uncinate process of the pancreas and thyroid), elimination or another origin (e.g., inflammation, infection, and meningioma) was considered pathological. [68Ga]Ga-DOTA-TOC PET/CT was interpreted as positive at the patient level when at least 1 pathological focus was visualized.

In the 6 patients in whom 2-[18F]FDG and/or 6-[18F]FDOPA PET/CT had also been performed, we reported the number of
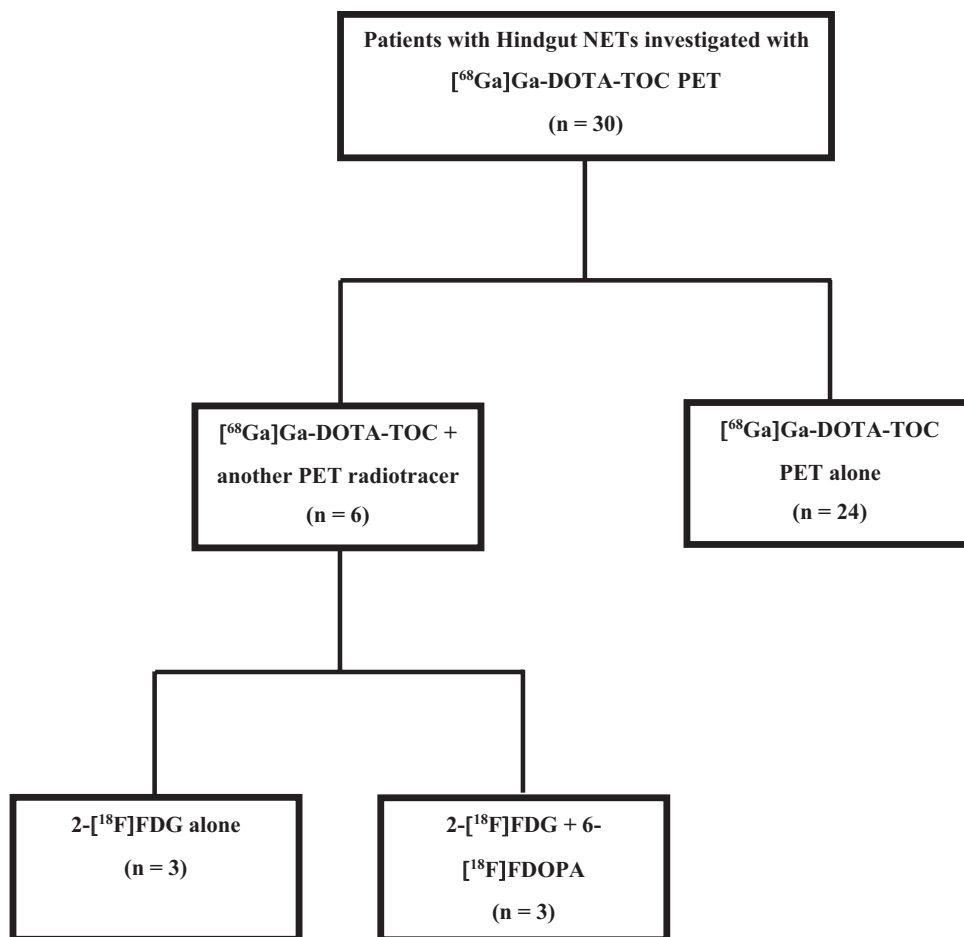
Figure 1. Flow diagram outlining the different PET radiotracers applied to the 30 patients with colorectal neuroendocrine tumors derived from hindgut.

foci with pathologically increased uptake detected and compared them on a site basis. For this intraindividual PET imaging comparison, 5 pathologic sites were considered: rectal primary tumor, liver, bone, pancreas and pelvic lymph nodes (PLNs). If more than 5 lesions were visualized within 1 site, the number of lesions was truncated at 5 for that site to avoid bias. To more precisely compare the results obtained with the 3 PET radiotracers, the intensity of uptake was determined by the semiquantitative index SUV_{max} by applying a spherical volume of interest drawn around pathological uptake foci. SUV_{max} was calculated by measuring the maximal concentration of radiotracer in the volume of interest corrected for body weight and injected activity. If several distinct pathological uptake foci were visualized in the same site, we kept the lesion with the highest SUV_{max} for comparison.

To study whether a correlation existed between [68Ga] Ga-DOTA-TOC PET/CT uptake and the Ki-67 proliferative index of the lesions, we measured on [68Ga]Ga-DOTA-TOC PET/CT the SUV_{max} of the site of tissue biopsy when available. For patients who underwent surgical resection of relevant lesions, we used [68Ga]Ga-DOTA-TOC PET/CT before resection.

2.3. Follow-up and evaluation of impact on patient disease management

After imaging, clinical follow-up was performed for each patient by the referring physician. Clinicians decided on a management plan for each patient during multidisciplinary team meetings. We defined the impact of [68Ga]Ga-DOTA-TOC PET/CT as any change in management decided by clinicians during the multidisciplinary meeting triggered by [68Ga]Ga-DOTA-TOC PET/CT. Management changes were classified as major or minor. An intermodality management change, defined as a management change between treatment modalities (e.g., from surgery to medical therapy or from no treatment to therapy), was classified as a major change. A minor change corresponded to an intramodality management change, defined as a management change within a treatment modality (e.g., change in chemotherapy regimen or change of surgical procedure) or a management change with no change in treatment (e.g., indication/no indication for biopsies or other diagnostic examinations).

2.4. Standard of truth

A composite standard of truth to evaluate the PET/CT results as a true positive (TP), true negative, false positive and false negative was based on all data that were available during the follow-up period: histological findings, the results of other imaging and clinical follow-up. Histological findings, when available, were considered trustworthy criteria.

2.5. Statistical analysis

Statistical analyses were performed using XLSTAT 2020.4.1 (Addinsoft, Paris, France). We considered a P value $< .05$ to be statistically significant. Pairwise comparisons of sensitivities of the different PET radiotracers on a lesion basis were performed by Fisher's exact test. Values of Ki-67 PI and SUV_{max} are reported as the median and interquartile range (IQR). The following parameters were normally distributed according to the

Kolmogorov–Smirnov test. Thus, the correlation between the values of Ki-67 PI and SUV_{max} of the same lesion was evaluated using Pearson's correlation coefficient.

3. Results

3.1. Patient characteristics

We excluded 2 patients with neuroendocrine carcinomas for whom 2-[18F]FDG was the reference PET radiopharmaceutical and 1 patient initially referred for a histologically proven rectal NET that was misdiagnosed and corresponded finally to a stromal tumor. Ultimately, thirty consecutive patients who met the inclusion criteria were retrospectively included, and their clinicopathologic features are presented in Table 1.

Of the 30 patients, 12 were females (40%). The median age at initial diagnosis was 55 years (range: 28–76 years old). The most common primary tumor site was the rectum, with a 9:1 rectum-to-sigmoid colon ratio. Based on the histology of primary tumors, 13 patients (43%) had a disease classified as NET G1, 16 patients (54%) had a disease classified as NET G2, and 1 patient (3%) had a disease classified as NET G3.

As presented in Table 2, patients were referred to our center for staging after an initial diagnosis of NET (11 examinations), suspicion of incomplete resection of the primary tumor (1 examination), suspicion of recurrence (5 examinations), restaging (5 examinations), selection for PRRT (4 examinations) and systematic follow-up after treatment (4 examinations).

The median duration of follow-up after [68Ga]Ga-DOTA-TOC PET/CT was 11 months (IQR, 3–24).

3.2. [68Ga]Ga-DOTA-TOC PET/CT results

Of the 30 patients, 20 (67%) were scanned on a Gemini TF16 (PET/CT 1), and 10 (33%) were scanned on a Biograph mCT-flow (PET/CT 2).

For the per-patient-based analysis, [68Ga]Ga-DOTA-TOC PET/CT was accurate in all patients with 20 TPs and 10 TNs (Table 2). The histologic proof was obtained for at least 1 lesion in 14 of 20 patients with a positive [68Ga]Ga-DOTA-TOC PET/CT result and in 1 patient with a negative [68Ga]Ga-DOTA-TOC PET/CT result (true negative confirmed histologically after biopsy of polypectomy scar in patient no. 25).

[68Ga]Ga-DOTA-TOC PET/CT correctly identified the primary tumor in all patients with primary tumor not resected before the examination and in the patient with incomplete primary resection (patient no. 28).

Away from the primary tumor, the tumor sites that most frequently exhibited pathological uptake were the liver (15/30 cases), bones (12/30 cases) and PLNs (16/30 cases). PLNs were notably detected in 7/11 of the patients referred for initial staging of the disease (patients no. 2, 3, 5, 9, 10, 19 and 27). Moreover, [68Ga]Ga-DOTA-TOC PET/CT enabled the diagnosis of unexpected distant metastases in 4/11 of these patients (unexpected liver metastases in patient no. 9; unexpected bone metastases in patients no. 2, 9 and 27; and unexpected spleen metastases (Fig. 2) in patient no. 17). In all patients with liver metastases diagnosed before [68Ga]Ga-DOTA-TOC PET/CT, this examination was positive for liver involvement. Extra pelvic lymph node involvement was rarely observed with a pathological uptake of abdominal and/or thoracic lymph nodes seen in only 3 cases (patients no. 8, 23, 30), all indications included.

Table 1

Patient characteristics.

Patient no.	Gender	Age at initial diagnosis (yrs)	Primary site	Histological grading (WHO 2019)	Primary excision before SR PET	Surgical margin status	PET/CT camera	Time interval between initial diagnosis and SR PET (mo)
1	M	47	Rectum	G1	Yes	R1	PET/CT 1	143
2	M	64	Rectum	G2	No	−	PET/CT 2	0
3	F	45	Rectum	G2	Yes	N/A	PET/CT 2	2
4	M	75	Rectum	G2	No	−	PET/CT 1	21
5	F	49	Rectum	G1	Yes	R0	PET/CT 1	4
6	M	43	Rectum	G2	Yes	R0	PET/CT 2	49
7	F	37	Rectum	G1	Yes	R0	PET/CT 1	7
8	M	58	Rectum	G2	Yes	R0	PET/CT 1	148
9	F	52	Rectum	G2	No	−	PET/CT 1	0
10	M	42	Rectum	G2	No	−	PET/CT 1	9
11	M	56	Rectum	G1	Yes	R0	PET/CT 2	12
12	M	50	Rectum	G1	Yes	R1	PET/CT 1	17
13	M	61	Rectum	G2	Yes	R0	PET/CT 2	5
14	F	53	Sigmoid colon	G1	Yes	R0	PET/CT 1	2
15	F	57	Sigmoid colon	G1	Yes	R0	PET/CT 2	25
16	M	65	Sigmoid colon	G2	Yes	N/A	PET/CT 1	41
17	F	50	Rectum	G1	No	−	PET/CT 2	5
18	M	67	Rectum	G1	Yes	R0	PET/CT 1	18
19	F	60	Rectum	G1	No	−	PET/CT 1	26
20	M	38	Rectum	G1	Yes	R0	PET/CT 1	74
21	F	44	Rectum	G2	Yes	R0	PET/CT 1	16
22	F	59	Rectum	G1	Yes	N/A	PET/CT 1	3
23	F	76	Rectum	G2	Yes	N/A	PET/CT 1	60
24	M	62	Rectum	G2	Yes	N/A	PET/CT 1	125
25	F	37	Rectum	G1	Yes	N/A	PET/CT 1	4
26	M	44	Rectum	G3 (Well diff tu; Ki-67 30%)	Yes	R0	PET/CT 1	12
27	M	28	Rectum	G2	No	−	PET/CT 1	2
28	M	66	Rectum	G2	Yes	R2	PET/CT 2	24
29	M	62	Rectum	G2	No	−	PET/CT 2	3
30	M	70	Rectum	G2	No	−	PET/CT 2	38

F = female, M = male, N/A = not available, R0 = no microscopic residual tumor, R1 = microscopic residual tumor, R2 = macroscopic residual tumor, SR = somatostatin receptors, Well diff tu = well-differentiated tumor, WHO = World Health Organization; − = no surgery done.

Table 2

Results of [⁶⁸Ga]Ga-DOTA-TOC PET/CT on a per-patient basis.

| Patient no.	Indication to perform SR-PET	Context	[⁶⁸Ga]Ga-DOTA-TOC PET/CT result	Reference	Tumour sites identified
1	Restaging	Before planned liver transplant	TP	Histology	*Liver, PLN
2	Staging	Rectal NET with hepatic lesions seen on CI	TP	Histology	*Primary, *Liver, PLN, Bones
3	Staging	After resection of the primary tumor	TP	Follow-up	PLN
4	Selection for PRRT	Progression of hepatic and bone metastases after systemic treatments	TP	Histology	*Primary, Liver, PLN, Bones
5	Staging	After resection of a 6 mm rectal NET	TP	Histology	*PLN
6	Restaging	Doubtful image of the pancreatic tail (NET or adenocarcinoma?) seen on CI in a context of metastatic NET	TP	Histology	*Liver, Bones, *Pancreas
7	Suspicion of recurrence	Characterization of pelvic lymph nodes seen on echography	TN	Follow-up	–
8	Restaging	Alteration of general condition in a context of treated metastatic NET	TP	Follow-up	ALN
9	Staging	After diagnosis of rectal NET	TP	Histology	*Primary, *Liver, PLN, Bones
10	Staging	After diagnosis of rectal NET with hepatic lesions seen on CI	TP	Histology	*Primary, *Liver, PLN
11	Systematic follow-up	Systematic search of residual disease 12 months after surgery	TN	Follow-up	–
12	Selection for PRRT	Progressive pelvic lymphadenopathy seen on CI, responsible for uncontrolled pain	TP	Follow-up	PLN
13	Staging	After resection of a large NET invading perirectal fat with hepatic and bone lesions seen on CI	TP	Follow-up	Liver, Bones
14	Staging	After resection of the primary tumor	TN	Follow-up	–
15	Systematic follow-up	Systematic search of residual disease 2 years after surgery	TN	Follow-up	–
16	Suspicion of recurrence	Characterization of hepatic lesions seen on CI	TP	Follow-up	Liver, PLN
17	Staging	After resection of rectal NET with hepatic and bone lesions seen on CI	TP	Histology	*Primary, Liver, Spleen, Bones
18	Systematic follow-up	Systematic search of residual disease 18 months after surgery	TN	Follow-up	–
19	Staging	After diagnosis of rectal NET with pelvic lymphadenopathy seen on CI	TP	Histology	*Primary, PLN
20	Suspicion of recurrence	Elevated CgA serum level associated with flush	TN	Follow-up	–
21	Suspicion of recurrence	Characterization of mesenteric lymph nodes seen on CI	TN	Follow-up	–
22	Staging	After resection of a 6 mm rectal NET	TN	Follow-up	–
23	Selection for PRRT	Progression of hepatic metastases after systemic treatments	TP	Follow-up	Liver, PLN, ALN, TLN, Bones
24	Suspicion of recurrence	Characterization of hepatic lesions seen on CI	TP	Histology	*Liver, PLN, Bones
25	Suspicion of incomplete resection of primary	After resection of a 6 mm rectal NET	TN	Histology	– (*Polypectomy scar)
26	Systematic follow-up	Systematic search of residual disease 12 months after surgery	TN	Follow-up	–
27	Staging	After diagnosis of rectal NET with hepatic lesions seen on CI	TP	Histology	*Primary, *Liver, PLN, Bones
28	Restaging	After 6 months of SSA treatment for multi-metastatic disease	TP	Histology	*Primary, Liver, PLN, Bones
29	Restaging	After 2 months of SSA treatment for liver metastases	TP	Histology	*Primary, Liver, PLN, Bones
30	Selection for PRRT	Disease progression after mTOR inhibitor therapy	TP	Histology	*Primary, *Liver, PLN, ALN, TLN, Bones, PL, Lung

ALN = abdominal lymph nodes, CgA = chromogranin A, CI = conventional imaging (including contrast-enhanced CT and/or MRI), mTOR = mammalian target of rapamycin, PL = peritoneal lesions, PLN = pelvic lymph nodes, PRRT = peptide receptor radionuclide therapy, SRS = somatostatin receptor scintigraphy, SSA = somatostatin analogue, TLN = thoracic lymph nodes, TN = true negative, TP = true positive; *histological record; – = no lesion found.

The grade of the hindgut NET, the primary tumor location (sigmoid colon or rectum) or the PET/CT machine used did not impact the diagnostic performance of [⁶⁸Ga]Ga-DOTA-TOC PET/CT.

3.3. Impact of [⁶⁸Ga]Ga-DOTA-TOC PET/CT on patient management

[⁶⁸Ga]Ga-DOTA-TOC PET/CT led to a management change in 17/30 (57%) patients (Supplemental Table, Supplemental Digital Content, http://links.lww.com/MD/H812). The management changes consisted of 12 major changes and 5 minor changes. The major intermodality changes were as follows: cancelation of previously planned liver transplant (patient no. 1), indication for SSA therapy (patients no. 2, 3, and 16), indication for a previously unplanned surgical operation (patients no. 5 and 9), indication for a chemotherapy (patient no. 10), validation of a PRRT project (patients no. 4, 12, 23 and 30) and indication for chemo-embolization of liver metastases (patient no. 24). The minor changes were intramodality management changes or changes in the diagnostic strategy. Indeed, negative [⁶⁸Ga]Ga-DOTA-TOC
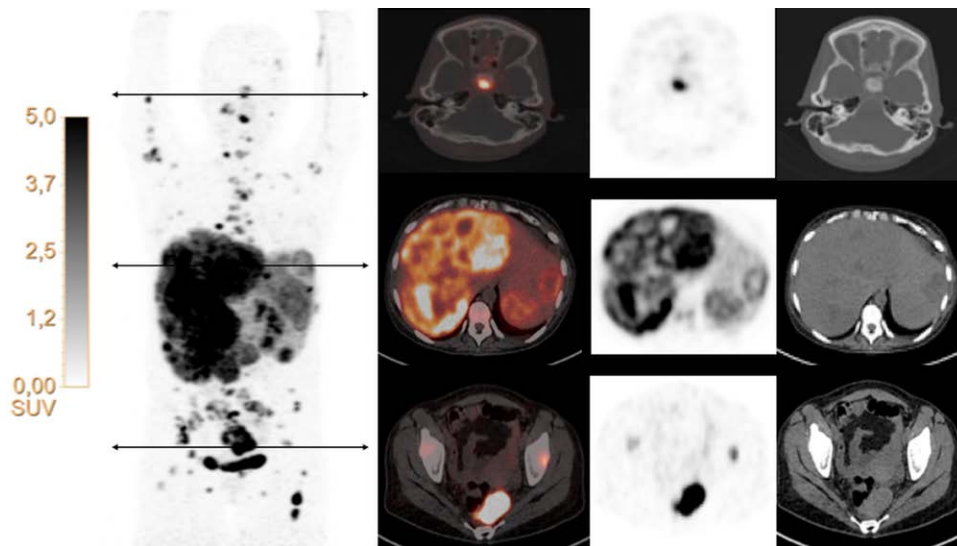
Figure 2. A 50-year-old woman (patient no. 17) was referred for initial staging after diagnosis of a rectal NET with liver and bone metastases seen on conventional imaging. [68Ga]Ga-DOTA-TOC PET/CT showed multiple liver metastases with variable uptake due to intralesional heterogeneity. Rectal primary presented an intense and homogeneous uptake. In addition to the known metastases, spleen metastases and some additional osteoblastic bone metastases were clearly depicted with [68Ga]Ga-DOTA-TOC PET/CT.
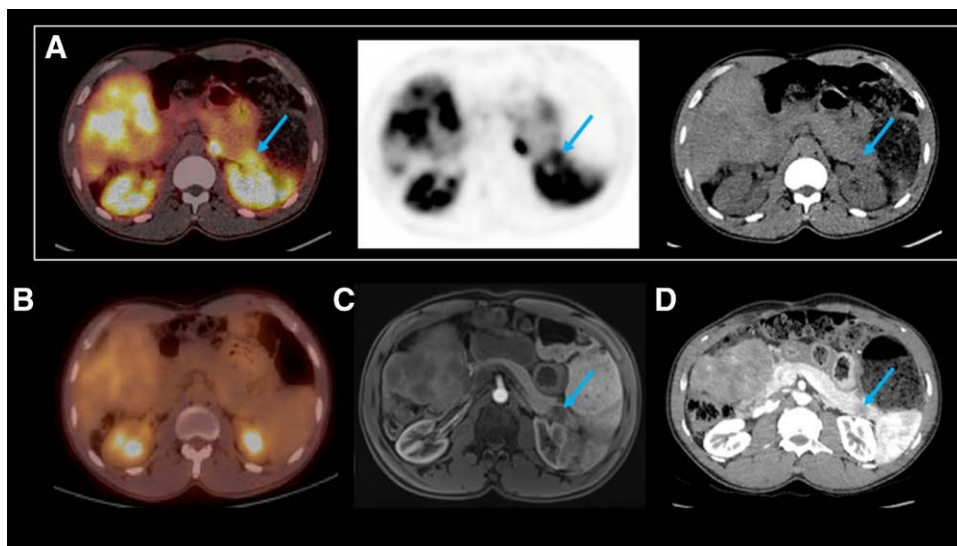
Figure 3. A 48-year-old man (patient no. 6) was referred to characterize a doubtful lesion of the pancreatic tail in the context of metastatic rectal NET. (A) Axial [68Ga]Ga-DOTA-TOC PET/CT images showed several liver metastases and a focus (SUV_{max} 9.8) localized at the tail of the pancreas (arrow), surrounded by areas of high physiological uptake in the spleen, left kidney and left adrenal. This lesion was slightly visible on the corresponding nonenhanced CT scan (arrow). (B) Axial 2-[18F]FDG PET/CT did not show pathological uptake at the pancreatic level. Axial gadolinium-enhanced T1-weighted fat saturated (C) and axial enhanced-CT scan (D) images clearly displayed atypical NET metastasis of the pancreatic tail, which was not enhanced at arterial time and subsequently confirmed by biopsy (arrows).

PET/CT results led to the cancelation of an unnecessary biopsy or complementary imaging in 4 patients (patients no. 7, 20, 21 and 25). All changes were retrospectively classified as pertinent apart from a case of inadequate minor change consisting of an unnecessary pancreatic biopsy. In this patient with multiple metastases (patient no. 6), a lesion localized at the tail of the pancreas was questionable, potentially consistent with adenocarcinoma. This lesion was misinterpreted as negative on the initial report, leading to a biopsy that revealed a NET. The retrospective reading corrected this misinterpretation (Fig. 3).

3.4. Comparison with 2-[18F]FDG and 6-[18F]FDOPA PET/CT

In the 6 patients in whom 2-[18F]FDG PET/CT (as well as 6-[18F]FDOPA PET/CT in 3 of them) had also been performed, a clear superiority of [68Ga]Ga-DOTA-TOC PET/CT over these 2 techniques was observed, especially at the lesion level, according to the number of lesions and to the intensity of uptake (Table 3).

3.4.1. Comparison with 2-[18F]FDG PET/CT. At the patient level, a TP was found by [68Ga]Ga-DOTA-TOC PET/CT in these 6 patients. A TP was found by 2-[18F]FDG in 5 of them, showing at least 1 lesion and false negative in 1 patient (patient no. 1), indicating a sensitivity of 83%.

On a lesion basis in these 6 patients, [68Ga]Ga-DOTA-TOC PET/CT detected 49 foci versus 18 on 2-[18F]FDG PET/CT, corresponding to a significant difference in sensitivity ($P < .05$; Fisher's exact test). Comparing [68Ga]Ga-DOTA-TOC PET/CT and 2-[18F]FDG PET/CT findings site by site, [68Ga]Ga-DOTA-TOC PET/CT identified more foci in the pelvic lymph nodes (10

Table 3

Comparison of lesion sites, number of lesions and SUV$_{max}$ values between [68Ga]Ga-DOTA-TOC, 2-[18F]FDG and 6-[18F]FDOPA PET/CT.

Patient no.	Lesion sites (Ki-67 PI)	[68Ga]Ga-DOTA-TOC: number of lesions	2-[18F]FDG: number of lesions	6-[18F]FDOPA: number of lesions	SUV$_{max}$ [68Ga]Ga-DOTA-TOC	SUV$_{max}$ 2-[18F]FDG	SUV$_{max}$ 6-[18F]FDOPA
1	Nodes	1	0	0	4.7	npu	npu
	*Liver (1%)	5	0	0	32.2	npu	npu
2	*Rectum (3%)	2	1	–	46.1	3.5	–
	Nodes	1	1	–	20.1	2.4	–
	*Liver (6%)	5	0	–	35.2	npu	–
	Bones	5	0	–	44.8	npu	–
3	Nodes	5	3	0	11.2	3.6	npu
4	*Rectum (15%)	1	1	0	31.8	4.6	npu
	Nodes	2	0	0	22.1	npu	npu
	Liver	5	5	0	44.7	7.5	npu
	Bones	5	5	5	43.5	7.2	5
5	*Nodes (1%)	1	1	–	56.1	8.9	–
6	*Liver (10%)	5	1	–	21.2	4	–
	Bones	5	0	–	16.9	npu	–
	*Pancreas (10%)	1	0	–	9.8	npu	–

npu = no pathological uptake, PI = proliferative index; * = histological record; – = not performed.

Table 4

Number of lesions detected by [68Ga]Ga-DOTA-TOC and 2-[18F]FDG PET/CT.

Lesion sites	[68Ga]Ga-DOTA-TOC PET/CT	2-[18F]FDG PET/CT
PLN	10	5
Liver	20	6
Bones	15	5
Pancreas	1	0
Rectum	3	2
Total	49	18

PLN = pelvic lymph nodes

vs. 5), liver (20 vs. 6), bones (15 vs. 5), pancreas (1 vs. 0) and rectum (3 vs. 2) (Table 4).

3.4.2. Comparison with 6-[18F]FDOPA PET/CT.
6-[18F]FDOPA PET/CT was positive in 1 of 3 patients (patient no. 4), showing a few bone lesions with a very low intensity of uptake and missing all other extraosseous lesions (primary tumor, lymph nodes and liver (Fig. 4)), indicating a sensitivity of 33%. On a lesion basis in patient no. 4, [68Ga]Ga-DOTA-TOC PET/CT detected 24 foci versus 5 on 6-[18F]FDOPA PET/CT, corresponding to a significant difference in sensitivity ($P < .05$; Fisher's exact test).

The SUV$_{max}$ values for each lesion detected with [68Ga]Ga-DOTA-TOC PET/CT, 2-[18F]FDG and 6-[18F]FDOPA PET/CT are reported in the previous Table 3. Comparing lesion by lesion, SUV$_{max}$ for [68Ga]Ga-DOTA-TOC PET/CT was clearly higher in all lesions.

### 3.5. Study of the relationship between the value of ki-67 PI and [68Ga]Ga-DOTA-TOC PET/CT uptake

There was no significant correlation between the Ki-67 PI and SUV$_{max}$ values among the 17 available lesions ($r = -0.15$, $P = .56$) (Fig. 5). Among these 17 lesions, 4 (24%) grade 1 samples had a median Ki-67 PI of 1% (IQR, 1–1) and median SUV$_{max}$ of 27.2 (IQR, 21.5–38.2), and 13 (76%) grade 2 samples had a median Ki-67 PI of 9% (IQR, 5–10) and median SUV$_{max}$ of 23.6 (IQR, 19.7–35,2). The subgroup analysis of an association between values of Ki-67 PI and SUV$_{max}$ within grade 2 samples was not significant ($r = -0.03$, $P = .95$) and could not be conducted for grade 1 samples due to an insufficient sample size (Table 5).

4. Discussion

To the best of our knowledge, the present study is the first to explore the diagnostic performance of [68Ga]Ga-DOTA-TOC PET/CT in the specific context of well-differentiated colorectal NETs deriving from the hindgut, including both rectal and colic NETs. Our results indicate the high performance of [68Ga]Ga-DOTA-TOC PET/CT, consistent with the known high performance of [68Ga]Ga-DOTA-TOC PET/CT and, more generally, of SR PET in well-differentiated NETs regardless of their origin. In this respect, 2 meta-analyses showed pooled sensitivities and specificities of [68Ga]Ga-DOTA-TOC PET/CT of 92% to 93% and 82% to 85%, respectively,[22,23] in different types of NETs.

The excellent diagnostic performance of [68Ga]Ga-DOTA-TOC PET/CT led to a change in management in 57% of patients, a proportion similar to that reported in the metanalysis of Graham et al.,[22] which considered all types of NETs. [68Ga]Ga-DOTA-TOC PET/CT greatly impacted management by allowing the identification of additional sites of disease when surgery with curative intent was considered and provided significant additional information compared with anatomic imaging. This additional information most commonly consisted of unexpected identification of disease in bone, liver, and nodal sites. The impact of SR PET in our study was pertinent in all cases except for a minor inadequate change in patient no. 6 for whom an initial misinterpretation of the [68Ga]Ga-DOTA-TOC PET/CT led to an unnecessary pancreatic biopsy. Our re-reading, performed with careful confrontation of [68Ga]Ga-DOTA-TOC PET/CT with contrast-enhanced abdominal CT and magnetic resonance imaging, allowed us to retrospectively correctly characterize this pancreatic lesion whose uptake was significant but of moderate intensity in a location (the tail of pancreas) surrounded by zones of high physiologic uptake, such as the spleen and kidney. This example emphasizes the value of comparing SR PET with highly specialized morphologic imaging techniques even if, globally, SR PET has been shown to be superior to anatomic imaging[24] for the detection of well-differentiated NETs.

Along with SR PET, NETs can be imaged by using PET with other radiopharmaceuticals. 2-[18F]FDG and 6-[18F]FDOPA are commonly used in nuclear medicine to study different aspects of tumor biology, such as glucose or amino acid metabolism. In the present paper, we conducted an intraindividual comparison of the results in the few patients who were also explored
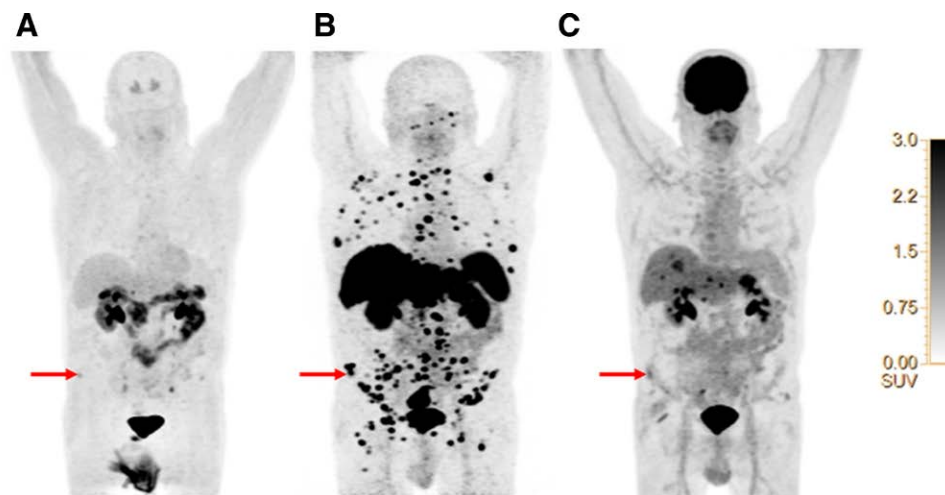
Figure 4. Anterior view of 3D maximum intensity projection PET images: 6-[18F]FDOPA (A), [68Ga]Ga-DOTA-TOC (B) and 2-[18F]FDG (C) PET images performed on a 77-year-old man (patient no. 4) for workup before the new treatment strategy of a progressive metastatic rectal NET. All 3 radiotracers identified lesions at the bone level (arrows). However, [68Ga]Ga-DOTA-TOC and 2-[18F]FDG PET identified many more lesions than 6-[18F]FDOPA. 6-[18F]FDOPA did not show extraosseous lesions. [68Ga]Ga-DOTA-TOC and 2-[18F]FDG PET identified the primary tumor and lesions at the liver level, while only [68Ga]Ga-DOTA-TOC identified lesions at the pelvic lymph node level. [68Ga]Ga-DOTA-TOC PET clearly showed a much more intense uptake than other radiotracers.
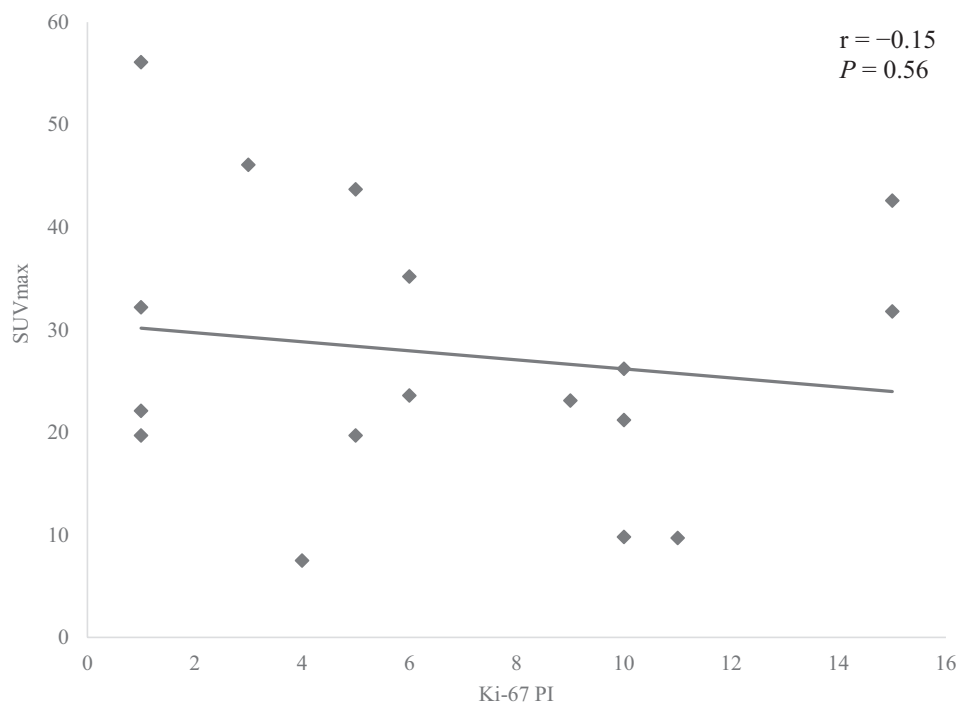
Figure 5. Relationship between Ki-67 and [68Ga]Ga-DOTA-TOC SUV_{max}. No correlation was demonstrated. The figure was prepared using XLSTAT (Addinsoft, New York, USA).

with 2-[18F]FDG and/or 6-[18F]FDOPA PET/CT. Overall, the diagnostic performance of [68Ga]Ga-DOTA-TOC PET/CT appeared to be superior to that of 2-[18F]FDG PET/CT. 2-[18F]FDG PET/CT identified only the same lesions detected on [68Ga]Ga-DOTA-TOC PET/CT with no additional tumor site. [68Ga]Ga-DOTA-TOC PET/CT was able to detect a higher number of lesions at the rectum, pelvic lymph node, bone and liver levels. Compared with 2-[18F]FDG PET/CT, [68Ga]Ga-DOTA-TOC had an extraordinary target-to-background contrast, reflected in high standardized uptake values, which were significantly greater than those seen with 2-[18F]FDG. Indeed, given the low metabolic rate of most well-differentiated NETs, standard PET imaging using 2-[18F]FDG is relatively ineffective, but positivity suggests a highly aggressive lesion and a worse prognosis.[25–27] Conversely, with the potential prognostic interest of a

Table 5

Matched Lesions—Ki-67 PI and SUV_{max}.

Histological grading (WHO 2019)	Total, n (%) (n = 17)	Ki-67 PI, Median (%) (IQR)	SUV_{max}, Median (IQR)	P
1	4 (24)	1 (1 – 1)	27.2 (21.5 – 38.2)	ns
2	13 (76)	9 (5 – 10)	23.6 (19.7 – 35,2)	.95

IQR = interquartile range, ns = not significant, PI = proliferative index, WHO = World Health Organization.

complementary PET exploration using 2-[18F]FDG, we found no interest in using 6-[18F]FDOPA, which has a very poor sensitivity for NETs derived from the hindgut, with the reservation of the very small number of patients in whom both examinations were performed. In digestive NETs, this poor sensitivity is also observed in NETs derived from the foregut, in contrast with the fact that 6-[18F]FDOPA PET/CT is an excellent tool in NETs derived from the midgut,[28] with a diagnostic performance sometimes better than that of SR-PET.[29]

Otherwise, we did not find any correlation between the values of Ki-67 PI and [68Ga]Ga-DOTA-TOC PET/CT SUV_{max}, which differs from the results of Chan et al.,[30] where an inverse correlation between the values of Ki-67 PI and SUV_{max} was observed in NETs. This might be explained by the low statistical power of our analysis.

The clinicopathological characteristics of our study population were comparable with those of large epidemiologic cohorts in terms of the male-to-female ratio, median age at initial diagnosis and proportion of colic and rectal NETs,[31–33] with a high predominance of rectal localization. The most represented histological grade in our study was grade 2, which differs significantly from the high predominance (95%) of grade 1 described by Kim et al.,[31] but the majority of the patients in our study were referred for extensive disease, although 93% of patients in the descriptive study by Kim et al.[31] had a localized disease.

We reported that lymph nodes were a common site for metastases, mainly in the pelvis with involvement of presacral nodes and nodes adjacent to the iliac arteriovenous system, a distribution corresponding to that described by Gut et al.[34] In this respect, it is interesting to note that this lymph node distribution appears to differ from that of foregut and midgut NETs, where lymph node involvement is more widespread, especially for midgut NETs with frequent involvement of supra-diaphragmatic lymph nodes.[29,35] In our series, hindgut NETs involved the supra-diaphragmatic lymph nodes in only 2/30 patients (patients no. 23 and 30) who were being followed for metastatic disease in the context of therapeutic failure. We also reported atypical splenic involvement in 1 patient referred for initial staging (patient no. 17) associated with synchronous multiple liver and bone metastases. NET metastases involving the spleen are extremely rare, with an estimated prevalence of 0.07%,[36] because reticulo-endothelial tissue creates an unfavorable environment for the growth and survival of tumor cells.[37,38] To our knowledge, splenic involvement has never been reported in hindgut NETs before. Splenic metastases may originate from the splenic artery, splenic vein or lymphatics, but here, we supposed a hematogenous origin considering the multiple associated visceral metastases. Last, we reported only 1 patient with pathological pulmonary uptake in our cohort, reflecting the lower potential of rectal NETs to invade the lungs compared with adenocarcinomas at this site, as previously shown.[39]

This study has several limitations. The first limitation, shared by most imaging studies addressing the search for metastatic disease, is the lack of sufficient histological proof for most of the suspected metastases. Indeed, verification of every lesion was not feasible and ethically justifiable in most of the cases due to the tumor load, so we chose to use a composite standard of truth based on follow-up data and histological findings, if available. The second limitation of this work is its retrospective design, especially for the analysis of the impact on patient management, which was measured indirectly based on multidisciplinary team meeting conclusions and not by questionnaires (before and after PET examination) addressed to referring clinicians. Another limitation is the small size of the sample; however, associated with the rarity of patients presently referred, access to SR-PET is still limited in terms of PET/CT machines and [68Ge]Ge/[68Ga]Ga radionuclide generators. Finally, another notable limitation of this work was the fact that most patients were referred for [68Ga]Ga-DOTA-TOC PET/CT after other imaging techniques had failed or had given insufficient results, preventing a real comparison between the performance of [68Ga]Ga-DOTA-TOC PET/CT and the performance of other imaging modalities.

5. Conclusion

[68Ga]Ga-DOTA-TOC PET/CT appears to be a high-performance imaging modality in the assessment of well-differentiated NETs originating from the hindgut with a pertinent impact on patient management. We suggest that [68Ga]Ga-DOTA-TOC PET/CT be employed as the first-choice nuclear medicine modality, possibly with 2-[18F]FDG PET/CT as a complementary method for its potential in evaluating the prognosis of the disease.

Author contributions

Conceptualization: Pierre Delabie, Éric Baudin, Françoise Montravers.
Data curation: Pierre Delabie, Éric Baudin.
Formal analysis: Pierre Delabie, Françoise Montravers.
Investigation: Pierre Delabie, Françoise Montravers.
Methodology: Pierre Delabie, Françoise Montravers.
Project administration: Pierre Delabie, Françoise Montravers.
Resources: Françoise Montravers.
Software: Françoise Montravers.
Supervision: Françoise Montravers.
Validation: Françoise Montravers.
Visualization: Éric Baudin, Olivia Hentic, Pauline Afchain, Timofei Rusu, Françoise Montravers.
Writing – original draft: Pierre Delabie.
Writing – review & editing: Pierre Delabie, Françoise Montravers.

References

[1] Anthony LB, Strosberg JR, Klimstra DS, et al. The NANETS consensus guidelines for the diagnosis and management of gastrointestinal neuroendocrine tumors (nets): well-differentiated nets of the distal colon and rectum. Pancreas. 2010;39:767–74.
[2] Merg A, Wirtzfeld D, Wang J, et al. Viability of endoscopic and excisional treatment of early rectal carcinoids. J Gastrointest Surg. 2007;11:893–7.
[3] Wang AY, Ahmad NA. Rectal carcinoids. Curr Opin Gastroenterol. 2006;22:529–35.
[4] Pavel M, Oberg K, Falconi M, et al. Gastroenteropancreatic neuroendocrine neoplasms: ESMO Clinical Practice Guidelines for diagnosis, treatment and follow-up. Ann Oncol. 2020;31:844–60.
[5] Ramage JK, De Herder WW, Delle Fave G, et al. ENETS consensus guidelines update for colorectal neuroendocrine neoplasms. Neuroendocrinology. 2016;103:139–43.
[6] Kong G, Grozinsky-Glasberg S, Hofman MS, et al. Highly favourable outcomes with peptide receptor radionuclide therapy (PRRT) for metastatic rectal neuroendocrine neoplasia (NEN). Eur J Nucl Med Mol Imaging. 2019;46:718–27.
[7] Kaemmerer D, Peter L, Lupp A, et al. Molecular imaging with (6)(8) Ga-SSTR PET/CT and correlation to immunohistochemistry of somatostatin receptors in neuroendocrine tumours. Eur J Nucl Med Mol Imaging. 2011;38:1659–68.
[8] Kulaksiz H, Eissele R, Rossler D, et al. Identification of somatostatin receptor subtypes 1, 2A, 3, and 5 in neuroendocrine tumours with subtype specific antibodies. Gut. 2002;50:52–60.

[9] Buchmann I, Henze M, Engelbrecht S, et al. Comparison of 68Ga-DOTATOC PET and 111In-DTPAOC (Octreoscan) SPECT in patients with neuroendocrine tumours. Eur J Nucl Med Mol Imaging. 2007;34:1617–26.

[10] Gabriel M, Decristoforo C, Kendler D, et al. 68Ga-DOTA-Tyr3-octreotide PET in neuroendocrine tumors: comparison with somatostatin receptor scintigraphy and CT. J Nucl Med. 2007;48:508–18.

[11] Treglia G, Castaldi P, Rindi G, et al. Diagnostic performance of Gallium-68 somatostatin receptor PET and PET/CT in patients with thoracic and gastroenteropancreatic neuroendocrine tumours: a meta-analysis. Endocrine. 2012;42:80–7.

[12] Hoegerle S, Altehoefer C, Ghanem N, et al. Whole-body 18F dopa PET for detection of gastrointestinal carcinoid tumors. Radiology. 2001;220:373–80.

[13] Adams S, Baum R, Rink T, et al. Limited value of fluorine-18 fluorode-oxyglucose positron emission tomography for the imaging of neuroendocrine tumors. Eur J Nucl Med. 1998;25:79–83.

[14] Belhocine T, Foidart J, Rigo P, et al. Fluorodeoxyglucose positron emission tomography and somatostatin receptor scintigraphy for diagnosing and staging carcinoid tumours: correlations with the pathological indexes p53 and Ki-67. Nucl Med Commun. 2002;23:727–34.

[15] Sundin A, Eriksson B, Bergstrom M, et al. PET in the diagnosis of neuroendocrine tumors. Ann N Y Acad Sci. 2004;1014:246–57.

[16] Bozkurt MF, Virgolini I, Balogova S, et al. Guideline for PET/CT imaging of neuroendocrine neoplasms with (68)Ga-DOTA-conjugated somatostatin receptor targeting peptides and (18)F-DOPA. Eur J Nucl Med Mol Imaging. 2017;44:1588–601.

[17] Hope TA, Bergsland EK, Bozkurt MF, et al. Appropriate usc Criteria for somatostatin receptor PET imaging in neuroendocrine tumors. J Nucl Med. 2018;59:66–74.

[18] NCCN clinical practice guidelines in oncology. Neuroendocrine and adrenal tumors. Version 2.2020. National Comprehensive Cancer Network Web site. Available at: https://www.nccn.org

[19] Zhou Z, Wang Z, Zhang B, et al. Comparison of 68Ga-DOTANOC and 18F-FDG PET-CT scans in the evaluation of primary tumors and lymph node metastasis in patients with Rectal Neuroendocrine Tumors. Front Endocrinol (Lausanne). 2021;12:727327.

[20] Nagtegaal ID, Odze RD, Klimstra D, et al. The 2019 WHO classification of tumours of the digestive system. Histopathology. 2020;76:182–8.

[21] Breeman WA, de Jong M, de Blois E, et al. Radiolabelling DOTA-peptides with 68Ga. Eur J Nucl Med Mol Imaging. 2005;32:478–85.

[22] Graham MM, Gu X, Ginader T, et al. (68)Ga-DOTATOC imaging of neuroendocrine tumors: a systematic review and metaanalysis. J Nucl Med. 2017;58:1452–8.

[23] Yang J, Kan Y, Ge BH, et al. Diagnostic role of Gallium-68 DOTATOC and Gallium-68 DOTATATE PET in patients with neuroendocrine tumors: a meta-analysis. Acta Radiol. 2014;55:389–98.

[24] Frilling A, Sotiropoulos GC, Radtke A, et al. The impact of 68Ga-DOTATOC positron emission tomography/computed tomography on the multimodal management of patients with neuroendocrine tumors. Ann Surg. 2010;252:850–6.

[25] Bahri H, Laurence L, Edeline J, et al. High prognostic value of 18F-FDG PET for metastatic gastroenteropancreatic neuroendocrine tumors: a long-term evaluation. J Nucl Med. 2014;55:1786–90.

[26] Binderup T, Knigge U, Loft A, et al. 18F-fluorodeoxyglucose positron emission tomography predicts survival of patients with neuroendocrine tumors. Clin Cancer Res. 2010;16:978–85.

[27] Frilling A, Akerstrom G, Falconi M, et al. Neuroendocrine tumor disease: an evolving landscape. Endocr Relat Cancer. 2012;19:R163–85.

[28] Montravers F, Grahek D, Kerrou K, et al. Can fluorodihydroxyphenyl-alanine PET replace somatostatin receptor scintigraphy in patients with digestive endocrine tumors? J Nucl Med. 2006;47:1455–62.

[29] Ouvrard E, Chevalier E, Addeo P, et al. Intraindividual comparison of (18) F-FDOPA and (68) Ga-DOTATOC PET/CT detection rate for metastatic assessment in patients with ileal neuroendocrine tumours. Clin Endocrinol (Oxf). 2021;94:66–73.

[30] Chan H, Moseley C, Zhang L, et al. Correlation of DOTATOC uptake and pathologic grade in neuroendocrine tumors. Pancreas. 2019;48:948–52.

[31] Kim ST, Ha SY, Lee J, et al. The Clinicopathologic features and treatment of 607 hindgut Neuroendocrine Tumor (NET) patients at a single institution. Medicine (Baltim). 2016;95:e3534.

[32] Shen C, Yin Y, Chen H, et al. Neuroendocrine tumors of colon and rectum: validation of clinical and prognostic values of the World Health Organization 2010 grading classifications and European Neuroendocrine Tumor Society staging systems. Oncotarget. 2017;8:22123–34.

[33] Zhang Y, Shang L, Zhang PP, et al. Clinicopathological features and prognostic validity of the European Neuroendocrine Tumor Society (ENETS) and American Joint Committee on Cancer (AJCC) 8th staging systems in colonic neuroendocrine neoplasms. Cancer Med. 2019;8:5000–11.

[34] Gut P, Waligorska-Stachura J, Czarnywojtek A, et al. Hindgut neuroendocrine neoplasms - characteristics and prognosis. Arch Med Sci. 2017;13:1427–32.

[35] Wang YZ, Mayhall G, Anthony LB, et al. Cervical and upper mediastinal lymph node metastasis from gastrointestinal and pancreatic neuroendocrine tumors: true incidence and management. J Am Coll Surg. 2012;214:1017–22.

[36] Carreras C, Kulkarni HR, Baum RP. Rare metastases detected by (68) Ga-somatostatin receptor PET/CT in patients with neuroendocrine tumors. Recent Results Cancer Res. 2013;194:379–84.

[37] Comperat E, Bardier-Dupas A, Camparo P, et al. Splenic metastases: clinicopathologic presentation, differential diagnosis, and pathogenesis. Arch Pathol Lab Med. 2007;131:965–9.

[38] Lam KY, Tang V. Metastatic tumors to the spleen: a 25-year clinicopathologic study. Arch Pathol Lab Med. 2000;124:526–30.

[39] Riihimaki M, Hemminki A, Sundquist K, et al. The epidemiology of metastases in neuroendocrine tumors. Int J Cancer. 2016;139:2679–86.